Analytical approach to localized structures in a simple reaction-diffusion system

Orazio Descalzi,[1,2] Yumino Hayase,[2,3] and Helmut R. Brand[2]
[1]*Facultad de Ingeniería, Universidad de los Andes, Santiago, Chile*
[2]*Department of Physics, University of Bayreuth, 95440 Bayreuth, Germany*
[3]*Department of Physics, Kyushu University, Fukuoka 812-8581, Japan*
(Received 29 July 2003; published 27 February 2004)

We study from an analytical point of view a simple reaction-diffusion model, which admits stable oscillating localized structures as a consequence of the coexistence between a stable limit cycle and a stable fixed point. Using a generalized matching approach we are able to find approximate analytical expressions for localized oscillating structures in this reaction-diffusion model capturing all the essential ingredients of these breathing particlelike solutions.

DOI: 10.1103/PhysRevE.69.026121 PACS number(s): 82.40.Ck, 82.40.Bj, 05.70.Ln

I. INTRODUCTION

Reaction-diffusion (RD) systems represent an important class of pattern-forming nonequilibrium systems [1] with applications in biology [2,3]. Experiments and computer simulations for RD systems show that pattern formation in the form of localized structures and pulse dynamics can lead to a rich variety of behavior.

One of the most interesting phenomena is self-replication, which has been observed in experiments [4,5] as well as in computer simulations [6–11].

The interaction of counterpropagating pulses is another interesting subject. Computer simulations of several reaction-diffusion systems have revealed that a propagating pulse can be stable upon collision with a counterpropagating pulse. By choosing suitable parameters in the system, they behave similar to elastic objects upon collision [12–15], or they are deformed during collisions but reemerge unchanged in size and shape well after the collision just like a soliton [16,17].

It is well known that bistable RD systems which possess two locally stable solutions and one unstable solution can show localized structures. Localized solutions are observed for systems with two stable fixed points and one unstable fixed point [18–20] or one stable fixed point, a stable limit cycle, and an unstable limit cycle. The latter systems show numerically localized structures which are similar to those in the quintic complex Ginzburg-Landau equation [16,21–23].

Localized solutions and their interactions have also been studied within the framework of envelope equations such as the quintic complex Ginzburg-Landau equation [24–33], order parameter equations including the quintic complex Swift-Hohenberg equation [34–36] and phase equations [37–40]. More recently it has been shown for in the quintic complex Ginzburg-Landau equation, that using a simple matching approach, for which one calculates the localized structure inside and outside the core and then matches the approximate solutions at the boundary of the regions, it is possible to study the mechanism of the appearance of pulses [41,42]. The aim of this paper is to generalize the above mentioned method in order to study analytically localized solutions in a simple RD system, which admits stable oscillating localized structures as a consequence of the coexistence between a stable limit cycle and a stable fixed point.

II. THE MODEL

The reaction-diffusion model we study has the form

$$u_t = \mu_1 u - \mu_2 v + \beta_r u^3 + \gamma_r u^5 + u_{xx}, \tag{1}$$

$$v_t = \mu_2 u + \mu_3 v + \beta_i u^3 + D v_{xx}, \tag{2}$$

where the indices x and t stand for derivatives with respect to the variables x and t, respectively. The system has the symmetry $u \to -u$ and $v \to -v$ simultaneously, but not separately. We take $\beta_r > 0$ (the cubic term does not saturate the motion), $\gamma_r < 0$ (the quintic term leads to saturation), a choice which guarantees stability for large values of u. Due to the term $\sim u^3$ in Eq. (2) the system is nonvariational. Replacing this term by a term $\sim uv^2$ in Eq. (2) or by terms of the type $\sim v^3$ or $\sim u^2 v$ in Eq. (1) leads also to nonvariational systems and to similar results. For simplicity we consider $D = 1$. Moreover, we are interested in the situation where the system (1) and (2) admits the coexistence between a stable fixed point ($u = v = 0$) and a stable limit cycle. In this case a typical plot of the null-clines and the limit cycle of the dynamical system (without spatial degrees of freedom) is shown in Fig. 1.

The reaction-diffusion model studied has been chosen such that the dynamical system associated with Eqs. (1) and (2) has the possibility to show *simultaneously* a stable fixed point and a stable limit cycle. This structural situation, which is sketched in Fig. 1, arises frequently for reaction-diffusion systems. It is also of direct importance to experimental studies in the field of autocatalytic chemical reactions (compare, for example, Ref. [43]).

In order to set up an analytical approach of the system (1) and (2) it is convenient to introduce a change of variables $(u,v) \to (R,\varphi)$, where $u = R\cos\varphi$ and $v = R\sin\varphi$. Writing $\varphi = \Omega t + \theta(x,t)$, where Ω is related to the oscillatory nature of the system and is an unknown parameter to be determined, the change of variables reads

$$u(x,t) = R(x,t)\cos[\Omega t + \theta(x,t)], \tag{3}$$

$$v(x,t) = R(x,t)\sin[\Omega t + \theta(x,t)]. \tag{4}$$

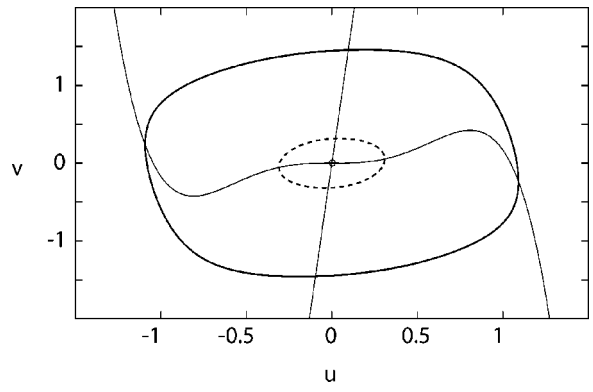

FIG. 1. A typical plot of the null-clines and the stable and unstable limit cycle of the dynamical system (without spatial degrees of freedom). The null-clines are shown as solid black lines. The origin of the u-v plane corresponds to a stable fixed point. The thick solid black line is a stable limit cycle, while the unstable limit cycle is shown as a dashed line. Parameters are $\mu_1=0$, $\mu_2=1.5$, $\mu_3=-0.2$, $\beta_r=3$, $\gamma_r=-2.75$, and $\beta_i=1.6$.

Inserting Eqs. (3) and (4) in Eqs. (1) and (2), we obtain the following equations for R and θ:

$$R_t-\frac{R}{2}(\mu_1+\mu_3)-R_{xx}+R\theta_x^2-\frac{3}{8}\beta_r R^3-\frac{5}{16}\gamma_r R^5 = \frac{R}{2}(\mu_1-\mu_3)\cos 2\varphi+\frac{\beta_r}{2}R^3\left(\cos 2\varphi+\frac{1}{4}\cos 4\varphi\right) + \frac{\beta_i}{4}R^3\left(\sin 2\varphi+\frac{1}{2}\sin 4\varphi\right)+\frac{\gamma_r}{16}R^5 \times(7\cos 2\varphi+3\cos 4\varphi+\cos 2\varphi\cos 4\varphi), \quad (5)$$

$$(\Omega+\theta_t)R-\mu_2 R-2R_x\theta_x-R\theta_{xx}-\frac{3}{8}\beta_i R^3 = \frac{R}{2}(\mu_3-\mu_1)\sin 2\varphi+\frac{\beta_i}{2}R^3\left(\cos 2\varphi+\frac{1}{4}\cos 4\varphi\right) - \frac{\beta_r}{4}R^3\left(\sin 2\varphi+\frac{1}{2}\sin 4\varphi\right)-\frac{\gamma_r}{8}R^5 \times\left(\frac{3}{2}\sin 2\varphi+\sin 4\varphi+\frac{1}{2}\sin 2\varphi\cos 4\varphi\right). \quad (6)$$

Equations (5) and (6) have the following form:

$$R_t-\frac{R}{2}(\mu_1+\mu_3)-R_{xx}+R\theta_x^2-\frac{3}{8}\beta_r R^3-\frac{5}{16}\gamma_r R^5=F(R,\varphi), \quad (7)$$

$$(\Omega+\theta_t)R-\mu_2 R-2R_x\theta_x-R\theta_{xx}-\frac{3}{8}\beta_i R^3=G(R,\varphi). \quad (8)$$

$F(R,\varphi)$ and $G(R,\varphi)$ are written as

$$F(R,\varphi)=F_{2\varphi}^{(1)}\sin 2\varphi+F_{2\varphi}^{(2)}\cos 2\varphi+\text{h.o.t}, \quad (9)$$

$$G(R,\varphi)=G_{2\varphi}^{(1)}\sin 2\varphi+G_{2\varphi}^{(2)}\cos 2\varphi+\text{h.o.t}, \quad (10)$$

where h.o.t stands for nonresonant higher-order terms of the form $\sin 4\varphi$, $\cos 4\varphi$, $\sin 2\varphi\cos 4\varphi$, or $\cos 2\varphi\cos 4\varphi$. The existence of the functions $F(R,\varphi)$ and $G(R,\varphi)$ is related to the absence of rotational symmetry, and thus the limit cycle is not a circle. Nevertheless we can consider these functions as a small perturbation of the perfect system (rotational symmetry). We consider formally $F(R,\varphi)$ and $G(R,\varphi)$ as being of order ϵ.

Thus we can proceed in a perturbation series

$$R(x,t)=R_0(x,t)+\epsilon R_1(x,t)+O(\epsilon^2), \quad (11)$$

$$\theta(x,t)=\theta_0(x,t)+\epsilon\theta_1(x,t)+O(\epsilon^2). \quad (12)$$

III. ZERO-ORDER PERTURBATION

At zero-order approximation $F(R,\varphi)=G(R,\varphi)=0$ and Eqs. (5) and (6) reduce to

$$R_{0t}=\mu R_0+\tfrac{3}{8}\beta_r R_0^3+\tfrac{5}{16}\gamma_r R_0^5+R_{0xx}-R_0\theta_{0x}^2, \quad (13)$$

$$R_0\theta_{0t}=(\mu_2-\Omega)R_0+\tfrac{3}{8}\beta_i R_0^3+2R_{0x}\theta_{0x}+R_0\theta_{0xx}, \quad (14)$$

where $\mu\equiv\frac{1}{2}(\mu_1+\mu_3)$. Defining $\varphi_0\equiv(\Omega-\mu_2)t+\theta_0(x,t)$ and $\psi_0\equiv R_0(x,t)e^{i\varphi_0(x,t)}$, Eqs. (13) and (14) are equivalent to a subcritical complex Ginzburg-Landau equation with no dispersive terms,

$$\psi_{0t}=\mu\psi_0+\tfrac{3}{8}(\beta_r+i\beta_i)|\psi_0|^2\psi_0+\tfrac{5}{16}\gamma_r|\psi_0|^4\psi_0+\psi_{0xx}. \quad (15)$$

At this order we can see that the parameter β_i is responsible for pulling out the system from the variational world. In fact, for $\beta_i=0$ Eq. (15) reduces to a real subcritical Ginzburg-Landau equation, which is variational. Therefore, for $\beta_i=0$, the above equation has a Maxwell point μ_M, which in terms of μ_1 and μ_3 leads to a Maxwell line for our original system (1) and (2):

$$\mu_1+\mu_3=\frac{27\beta_r^2}{160\gamma_r}. \quad (16)$$

It is well known that Eq. (15) has stable localized structures with R_0 and φ_{0x} not depending on time. Then Eqs. (13) and (14) can be written in the following form:

$$0=\mu R_0+\tfrac{3}{8}\beta_r R_0^3+\tfrac{5}{16}\gamma_r R_0^5+R_{0xx}-R_0\theta_{0x}^2, \quad (17)$$

$$(\Omega-\mu_2)R_0=\tfrac{3}{8}\beta_i R_0^3+2R_{0x}\theta_{0x}+R_0\theta_{0xx}. \quad (18)$$

It has been shown by Descalzi *et al.* [41,42] that it is possible to obtain analytical approximations for $R_0(x)$, θ_{0x}, and Ω. To solve Eqs. (17) and (18) we proceed to divide the x axis in a core region $\mathcal{R}_1$ and a region $\mathcal{R}_2$ outside the core of the pulse, and then we perform a matching.

In $\mathcal{R}_1$ we assume that the modulus $R_0(x)$ and the phase gradient $\theta_{0x}(x)$ admit Taylor expansions. We write

$$R_0(x)=R_m-\eta x^2+O(x^4), \quad (19)$$

where R_m is the largest value of $R_0(x)$, our second unknown (the first unknown is Ω). The expansion of the phase gradient reads

$$\theta_{0x}(x) = -\alpha x + O(x^3). \tag{20}$$

Inserting $R_0(x)$ and $\theta_{0x}(x)$ in Eqs. (17) and (18) we obtain

$$\eta = \frac{1}{2}\left(\mu R_m + \frac{3}{8}\beta_r R_m^3 + \frac{5}{16}\gamma_r R_m^5\right),$$

$$\alpha = \tfrac{3}{8}\beta_i R_m^2 - \Omega + \mu_2. \tag{21}$$

Outside the core of the pulse, in the region $\mathcal{R}_2$, we suppose that the phase gradient $\theta_{0x}(x)$ is determined by $\theta_{0x}(x)=p$ for $x<0$ and $\theta_{0x}(x)=-p$ for $x>0$. Since $R_0(x)$ goes asymptotically to zero, Eqs. (17) and (18) for $|x|\to\infty$ lead to

$$\Omega = \mu_2 + 2p\sqrt{-\mu+p^2}. \tag{22}$$

We see then that the frequency Ω is related to p and we remain finally with two unknowns: R_m and p. Solving Eq. (17) in $\mathcal{R}_2$, where the phase gradient is constant, we obtain

$$R_0(x) = \frac{2b^{1/4}\exp\{\sqrt{-\mu+p^2}(|x|+x_0)\}}{\sqrt{\left(\exp\{2\sqrt{-\mu+p^2}(|x|+x_0)\}+\dfrac{a}{\sqrt{b}}\right)^2-4}}, \tag{23}$$

where $a=-9\beta_r/5\gamma_r$, $b=-48(-\mu+p^2)/5\gamma_r$, and x_0 is a constant to be determined. The next step is to match $R_0(x)$ in regions $\mathcal{R}_1$ and $\mathcal{R}_2$. This is done at the point $(x_*,r_c) \equiv (-p/\alpha, R_m-\eta x_*^2)$ which has an obvious geometrical interpretation: r_c is the value of $R_0(x)$ at the matching point $x_*=-p/\alpha$ which is such that

$$\theta_{0x}=p \quad (x<x_*), \quad \theta_{0x}=-p \quad (x>-x_*);$$

$$\theta_{0x}=-\alpha x, \quad x\in\left[-\frac{p}{\alpha},\frac{p}{\alpha}\right]. \tag{24}$$

Using Eq. (23) we obtain

$$u_*^2 = -\frac{a}{\sqrt{b}} + \frac{2\sqrt{b}}{r_c^2} + \frac{2}{r_c^2}\sqrt{r_c^4 - a r_c^2 + b}, \tag{25}$$

where $u_*=\exp\{-\sqrt{-\mu+p^2}(x_*-x_0)\}$. Then

$$x_0 = x_* + \frac{\ln u_*}{\sqrt{-\mu+p^2}}. \tag{26}$$

We match now the derivative $dR_0(x)/dx$ at the same point x_*. From $R_0(x)$ outside the core in region $\mathcal{R}_2$ we get

$$\left(\frac{dR_0(x)}{dx}\right)_{x=x_*-0} = -\sqrt{-\mu+p^2}\left(r_c - \frac{r_c^3\left(u_*^2+\dfrac{a}{\sqrt{b}}\right)}{2\sqrt{b}}\right), \tag{27}$$

and inside the core, in region $\mathcal{R}_1$, the derivative reads

$$\left(\frac{dR_0(x)}{dx}\right)_{x=x_*+0} = -2\eta x_*. \tag{28}$$

Equating Eqs. (27) and (28) we get the first relation between R_m and p which reads

$$f(R_m,p) \equiv \sqrt{-\frac{5\gamma_r}{48}}\, r_c\sqrt{r_c^4 - a r_c^2 + b} + 2\eta x_* = 0. \tag{29}$$

We need a second relation in order to be able to fix the free parameters $\{R_m,p\}$. Multiplying Eq. (18) by $R_0(x)$ and integrating in the whole domain and since $R_0(x)$ is a symmetric function we obtain

$$g(R_m,p) \equiv \Omega - \mu_2 - \tfrac{3}{8}\beta_i \frac{\displaystyle\int_{-\infty}^{0} R_0^4 dx}{\displaystyle\int_{-\infty}^{0} R_0^2 dx} = 0. \tag{30}$$

The integrals in Eq. (30) can be evaluated and one gets

$$\int_{-\infty}^{0} R_0^2 dx = \frac{1}{2}\sqrt{-\frac{48}{5\gamma_r}}\ln\left|\frac{a+\sqrt{b}(u_*^2+2)}{a+\sqrt{b}(u_*^2-2)}\right| - R_m^2 x_* + \frac{2}{3}R_m\eta x_*^3. \tag{31}$$

$$\int_{-\infty}^{0} R_0^4 dx = -\sqrt{-\frac{48}{5\gamma_r}}\frac{(a^2-4b)\sqrt{b}+abu_*^2}{[-4b+(a+\sqrt{b}u_*^2)^2]} + \frac{a}{4}\sqrt{-\frac{48}{5\gamma_r}}\ln\left|\frac{a+\sqrt{b}(u_*^2+2)}{a+\sqrt{b}(u_*^2-2)}\right| - R_m^4 x_* + \frac{4}{3}R_m^3\eta x_*^3. \tag{32}$$

The existence of the curves $f(R_m,p)=0$ and $g(R_m,p)=0$ leads to the following scenario: There exists a critical value μ_{c1} so that for $\mu<\mu_{c1}$ the curves $f(R_m,p)=0$ and $g(R_m,p)=0$ do not intersect at any point suggesting there are no pulses [see Fig. 2(a)]. For $\mu>\mu_{c1}$ the curves intersect in two points giving rise to a stable and an unstable pulse via a saddle-node bifurcation [see Fig. 2(b)]. Notice that in Figs. 2(a) and 2(b) the curves $f=0$ and $g=0$ mean $\mathrm{Re}\, f=0$ and $\mathrm{Re}\, g=0$, respectively, because $\mathrm{Im}\, f=\mathrm{Im}\, g=0$ in the space (p,R_m).

By further increasing μ we find another critical value μ_{c2} so that for $\mu>\mu_{c2}$ there still exists an intersection between the curves $f=g=0$ (or $\mathrm{Re}\, f=\mathrm{Re}\, g=0$) predicting an un-

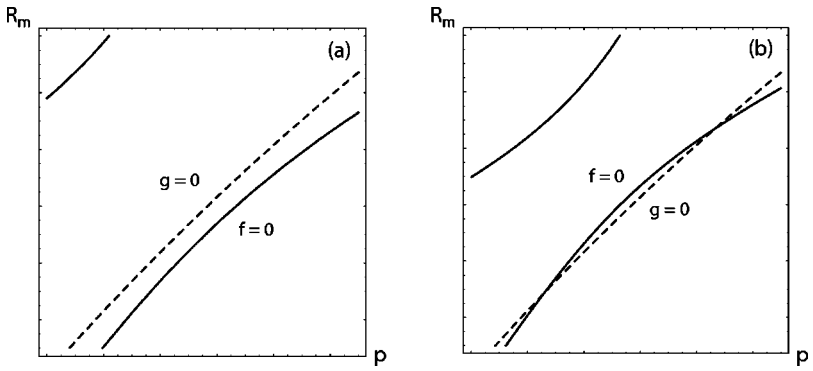

FIG. 2. (a) For $\mu<\mu_{c1}$ the curves $f(R_m,p)=0$ (continuous line) and $g(R_m,p)=0$ (dashed line) do not intersect at any point suggesting there are no pulses. (b) For $\mu>\mu_{c1}$ the curves intersect in two points giving rise to a stable and an unstable pulse via a saddle-node bifurcation.

stable pulse [see Fig. 3(a)], but the stable pulse disappears because there is no intersection between the curves $\mathrm{Re}\, f = \mathrm{Im}\, f = 0$ and $\mathrm{Re}\, g = \mathrm{Im}\, g = 0$ [see Fig. 3(b)]. This second bifurcation is associated with the appearance of fronts.

IV. PHASE DIAGRAM AT LEADING ORDER

According to the preceding section, for fixed parameters except μ, we have stable pulses for $\mu_{c1}<\mu<\mu_{c2}$. Thus stable pulses exist in the region limited by the lines $\mathcal{L}_1$ and $\mathcal{L}_2$ defined by $\mu_1=2\mu_{c1}-\mu_3$ and $\mu_1=2\mu_{c2}-\mu_3$, respectively. Moreover a linear stability analysis of the fixed point (0,0) of the system (1) and (2) leads to the following eigenvalues:

$$\lambda_{1,2}=\tfrac{1}{2}\{\mu_1+\mu_3\pm\sqrt{(\mu_1+\mu_3)^2-4(\mu_1\mu_3+\mu_2^2)}\}. \quad (33)$$

In order to obtain eigenvalues with negative real part we require $\mu_1+\mu_3<0$. In the quadrant where $\mu_1<0$ and $\mu_3>0$ we must require $\mu_1\mu_3>-\mu_2^2$ which is the region limited by the hyperbola $\mathcal{C}_1$: $\mu_1=-\mu_2^2/\mu_3$. In the quadrant where $\mu_1>0$ and $\mu_3<0$ we also demand $\mu_1\mu_3>-\mu_2^2$ which is the region limited by the hyperbola $\mathcal{C}_2$: $\mu_1=-\mu_2^2/\mu_3$. Thus, at this perturbation order, for fixed parameters except μ_1 and μ_3, we can divide the space $\mu_3-\mu_1$ in three parts: (i) A region where we can find stable pulses, which is limited by the lines $\mathcal{L}_1$, $\mathcal{L}_2$ and the hyperbolas $\mathcal{C}_1$ and $\mathcal{C}_2$ [see Fig. 4]; (ii) a region where all localized initial conditions lead to the stable solution zero. This region is that limited by $\mathcal{L}_1$ and the two hyperbolas; (iii) in the remaining space localized structures are unstable against front formation.

V. FIRST-ORDER PERTURBATION

Inserting Eqs. (11) and (12) into Eqs. (7) and (8) gives rise to the following equations for R_1 and θ_1:

$$\begin{aligned} &R_{1t}-\mu R_1-R_{1xx}\\ &\quad+2R_0\theta_{0x}\theta_{1x}+R_1\theta_{0x}^2-\frac{9}{8}\beta_r R_0^2R_1-\frac{25}{16}\gamma_r R_0^4R_1\\ &\quad=\frac{\Delta\mu}{2}R_0\cos 2\varphi+\frac{\beta_r}{2}R_0^3\cos 2\varphi+\frac{\beta_i}{4}R_0^3\sin 2\varphi\\ &\quad+\frac{7}{16}\gamma_r R_0^5\cos 2\varphi+O(\epsilon^2,\sin 4\varphi,\cos 4\varphi), \end{aligned} \quad (34)$$

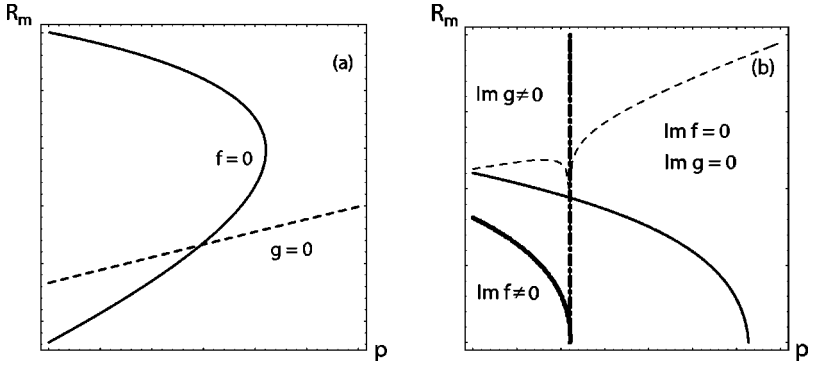

FIG. 3. For $\mu>\mu_{c2}$: (a) The intersection between the curves $f=0$ (continuous line) and $g=0$ (dashed line) still predicts a pulse (the unstable one). (b) There is no intersection between the curves $\mathrm{Re}\, f=\mathrm{Im}\, f=0$ and $\mathrm{Re}\, g=\mathrm{Im}\, g=0$ forbidding the existence of the other pulse (the stable one). The dot-dashed line separates the space (p,R_m) in two parts: $\mathrm{Im}\, g\neq 0$ and $\mathrm{Im}\, g=0$. Thick continuous line also separates the space (p,R_m) in two parts, namely, $\mathrm{Im}\, f\neq 0$ and $\mathrm{Im}\, f=0$. Thin continuous line means $\mathrm{Re}\, f=0$ and dashed line stands for $\mathrm{Re}\, g=0$.

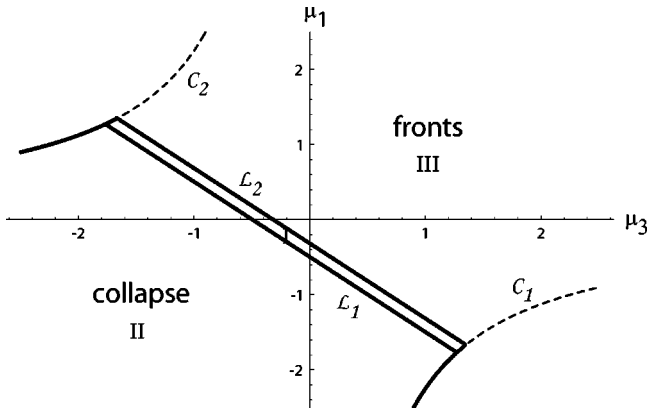

FIG. 4. Phase diagram for stable pulses at leading order. Parameters are $\mu_2=1.5$, $\beta_r=3$, $\gamma_r=-2.75$, and $\beta_i=1.0$.

$$(\Omega-\mu_2)R_1+R_0\theta_{1t}$$
$$-2R_{0x}\theta_{1x}-2R_{1x}\theta_{0x}-R_0\theta_{1xx}-R_1\theta_{0xx}-\frac{9}{8}\beta_i R_0^2 R_1$$
$$=-\frac{\Delta\mu}{2}R_0\sin 2\varphi+\frac{\beta_i}{2}R_0^3\cos 2\varphi-\frac{\beta_r}{4}R_0^3\sin 2\varphi$$
$$-\frac{3}{16}\gamma_r R_0^5\sin 2\varphi+O(\epsilon^2,\sin 4\varphi,\cos 4\varphi), \quad (35)$$

where $\Delta\mu\equiv\mu_1-\mu_3$. Now we proceed to solve the above equations outside and inside the core of the localized structure.

A. Outside the core

In order to solve Eqs. (34) and (35) outside the core, where $\theta_{0x}^2=p^2$, we make the following ansatz:

$$R_1=R_1^{(0)}+R_1^{(1)}+\text{h.o.t}, \quad (36)$$

$$\theta_1=\theta_1^{(0)}+\theta_1^{(1)}+\text{h.o.t}, \quad (37)$$

where h.o.t means terms $O(R_0^5)$, which are very small far away from the core of the pulse, and

$$R_1^{(0)}=R_0(\alpha_1\sin 2\varphi+\alpha_2\cos 2\varphi), \quad (38)$$

$$\theta_1^{(0)}=\beta_1\sin 2\varphi+\beta_2\cos 2\varphi, \quad (39)$$

$$R_1^{(1)}=R_0^3(\gamma_1\sin 2\varphi+\gamma_2\cos 2\varphi), \quad (40)$$

$$\theta_1^{(1)}=R_0^2(\epsilon_1\sin 2\varphi+\epsilon_2\cos 2\varphi). \quad (41)$$

Inserting Eqs. (36) and (37) into Eqs. (34) and (35) we obtain the following equations for $R_1^{(0)}$ and $\theta_1^{(0)}$:

$$R_{1t}^{(0)}+(p^2-\mu)R_1^{(0)}-R_{1xx}^{(0)}+2R_0p\theta_{1x}^{(0)}=\frac{\Delta\mu}{2}R_0\cos 2\varphi, \quad (42)$$

$$(\Omega-\mu_2)R_1^{(0)}+R_0\theta_{1t}^{(0)}-2R_{0x}\theta_{1x}^{(0)}-2R_{1x}^{(0)}p-R_0\theta_{1xx}^{(0)}$$
$$=-\frac{\Delta\mu}{2}R_0\sin 2\varphi. \quad (43)$$

Inserting expressions (38) and (39) into the above equations leads to the following system for α_1, α_2, β_1, and β_2:

$$\mu_2\alpha_1+2p^2\alpha_2+2p^2\beta_1=\frac{\Delta\mu}{4},$$
$$2p^2\alpha_1-\mu_2\alpha_2-2p^2\beta_2=0, \quad (44)$$

and

$$2p^2\beta_1-\mu_2\beta_2+2p^2\alpha_2=-\frac{\Delta\mu}{4},$$
$$\mu_2\beta_1+2p^2\beta_2-2p^2\alpha_1=0. \quad (45)$$

System Eq. (44) leads to

$$\alpha_1=\frac{1}{(\mu_2^2+4p^4)}\left(\mu_2\frac{\Delta\mu}{4}-2p^2\mu_2\beta_1+4p^4\beta_2\right),$$
$$\alpha_2=\frac{1}{(\mu_2^2+4p^4)}\left(p^2\frac{\Delta\mu}{2}-4p^2\beta_1-2p^2\mu_2\beta_2\right). \quad (46)$$

From Eq. (45) we finally get $\alpha_1=\beta_2=\Delta\mu/4\mu_2$, $\alpha_2=\beta_1=0$.

Thus we have determined $R_1^{(0)}(x,t)$ and $\theta_1^{(0)}(x,t)$:

$$R_1^{(0)}(x,t)=\frac{\Delta\mu}{4\mu_2}R_0(x)\sin 2[\Omega t+\theta_0(x)], \quad (47)$$

$$\theta_1^{(0)}(x,t)=\frac{\Delta\mu}{4\mu_2}\cos 2[\Omega t+\theta_0(x)]. \quad (48)$$

To obtain equations for $R_1^{(1)}$ and $\theta_1^{(1)}$ we proceed as before inserting expressions (36) and (37) into Eqs. (34) and (35). Thus we get

$$R_{1t}^{(1)}+(p^2-\mu)R_1^{(1)}-R_{1xx}^{(1)}+2R_0p\theta_{1x}^{(1)}-\frac{9}{8}\beta_r R_0^2 R_1^{(0)}$$
$$=\frac{\beta_r}{2}R_0^3\cos 2\varphi+\frac{\beta_i}{4}R_0^3\sin 2\varphi, \quad (49)$$

$$(\Omega-\mu_2)R_1^{(1)}+R_0\theta_{1t}^{(1)}-2R_{0x}\theta_{1x}^{(1)}-2R_{1x}^{(1)}p-R_0\theta_{1xx}^{(1)}$$
$$-\frac{9}{8}\beta_r R_0^2 R_1^{(0)}$$
$$=\frac{\beta_i}{2}R_0^3\cos 2\varphi-\frac{\beta_r}{4}R_0^3\sin 2\varphi. \quad (50)$$

Using the expressions for $R_1^{(0)}$, $R_1^{(1)}$, and $\theta_1^{(1)}$ given by Eqs. (38), (40), and (41) in Eq. (49) we obtain the following system:

$$\gamma_1(4\mu-2p^2)+\gamma_2(2\Omega-3\mu_2) = \frac{\beta_i}{8}+\frac{9}{16}\beta_r\alpha_1-(\Omega-\mu_2)\epsilon_1+2p^2\epsilon_2,$$

$$\gamma_1(3\mu_2-2\Omega)+\gamma_2(4\mu-2p^2)=\frac{\beta_r}{4}-(\Omega-\mu_2)\epsilon_2-2p^2\epsilon_1. \quad (51)$$

From the above system we get γ_1 and γ_2 in terms of ϵ_1 and ϵ_2:

$$\gamma_1=A_{00}+A_{01}\epsilon_1+A_{02}\epsilon_2,$$

$$\gamma_2=B_{00}+B_{01}\epsilon_1+B_{02}\epsilon_2, \quad (52)$$

where $A_{00}=(1/\Delta_1)[(4\mu-2p^2)(\beta_i/8+\frac{9}{16}\beta_r\alpha_1)+(3\mu_2-2\Omega)(\beta_r/4)]$, $A_{01}=(1/\Delta_1)[(\Omega-\mu_2)(2p^2-4\mu)+2p^2(2\Omega-3\mu_2)]$, $A_{02}=(1/\Delta_1)[2p^2(4\mu-2p^2)+(\Omega-\mu_2)(2\Omega-3\mu_2)]$, $B_{00}=(1/\Delta_1)[(2\Omega-3\mu_2)(\beta_i/8+\frac{9}{16}\beta_r\alpha_1)+(2\mu-p^2)(\beta_r/2)]$, $B_{01}=-A_{02}$, $B_{02}=A_{01}$, $\Delta_1=(4\mu-2p^2)^2+(2\Omega-3\mu_2)^2$.

To obtain a second relation between γ_1, γ_2, ϵ_1, and ϵ_2 we insert Eqs. (38), (40), and (41) into Eq. (50). Thus we get

$$\epsilon_1(4\mu-2p^2)+\epsilon_2(2\Omega-3\mu_2)-\gamma_1(\Omega-\mu_2)+2p^2\gamma_2 = \frac{9}{16}\beta_i\alpha_1-\frac{\beta_r}{8},$$

$$\epsilon_1(3\mu_2-2\Omega)+\epsilon_2(4\mu-2p^2)-2p^2\gamma_1-\gamma_2(\Omega-\mu_2)=\frac{\beta_i}{4}. \quad (53)$$

Inserting expressions (52) into Eq. (53) gives ϵ_1 and ϵ_2 as

$$\epsilon_1=\frac{1}{C_1^2+C_2^2}(C_1D_1-C_2D_2),$$

$$\epsilon_2=\frac{1}{C_1^2+C_2^2}(C_1D_2+C_2D_1), \quad (54)$$

where $C_1=4\mu-2p^2+(\mu_2-\Omega)A_{01}+2p^2B_{01}$, $C_2=2\Omega-3\mu_2+(\mu_2-\Omega)A_{02}+2p^2B_{02}$, $D_1=A_{00}(\Omega-\mu_2)-2p^2B_{00}+\frac{9}{16}\beta_i\alpha_1-\beta_r/8$, $D_2=\beta_i/4+2p^2A_{00}+(\Omega-\mu_2)B_{00}$.

Thus we have determined completely $R_1^{(1)}(x,t)$ and $\theta_1^{(1)}(x,t)$.

B. Inside the core

Taking into account that at zero order $R_0(x)=R_m-\epsilon x^2+O(x^4)$ and $\theta_{0x}(x)=-\alpha x+O(x^3)$ we can make the following ansatz for $R_1(x,t)$ and $\theta_1(x,t)$:

$$R_1(x,t)=(\gamma_{10}-\gamma_{11}x^2)\sin 2\varphi+(\gamma_{20}-\gamma_{21}x^2)\cos 2\varphi + O(x^4), \quad (55)$$

$$\theta_1(x,t)=(\delta_{10}+\delta_{11}x^2)\sin 2\varphi+(\delta_{20}+\delta_{21}x^2)\cos 2\varphi+O(x^4). \quad (56)$$

Inserting these expressions into Eqs. (34) and (35) we obtain the following set of equations:

$$\gamma_{11}=\frac{\beta_i}{8}R_m^3+\frac{\gamma_{10}}{2}\left(\mu+\frac{9}{8}\beta_rR_m^2+\frac{25}{16}\gamma_rR_m^4\right)+\gamma_{20}(\Omega+\alpha), \quad (57)$$

$$\gamma_{21}=\frac{\Delta\mu}{4}R_m+\frac{\beta_r}{4}R_m^3+\frac{7}{32}\gamma_rR_m^5-\gamma_{10}(\Omega+\alpha) + \frac{\gamma_{20}}{2}\left(\mu+\frac{9}{8}\beta_rR_m^2+\frac{25}{16}\gamma_rR_m^4\right), \quad (58)$$

$$\delta_{11}=\frac{\Delta\mu}{4}+\frac{\beta_r}{8}R_m^2+\frac{3}{32}\gamma_rR_m^4-\delta_{20}(\Omega+\alpha) + \frac{\gamma_{10}}{2R_m}\left(\Omega-\mu_2+\alpha-\frac{9}{8}\beta_iR_m^2\right), \quad (59)$$

$$\delta_{21}=\frac{\gamma_{20}}{2R_m}\left(\Omega-\mu_2+\alpha-\frac{9}{8}\beta_iR_m^2\right)+\delta_{10}(\Omega+\alpha)-\frac{\beta_i}{4}R_m^2. \quad (60)$$

VI. MATCHING APPROACH

System (57)–(60) has eight unknowns. The remaining equations are coming from the continuity of $R_1(x,t)$ and $\theta_{1x}(x,t)$ (calculated outside and inside the core of the pulse) at $x=x_*=-p/\alpha$.

A. Continuity of $R_1(x,t)$

Using $r_c\equiv R_0(x_*)=R_m-\eta x_*^2$, the continuity of $R_1(x,t)$ at $x=x_*$ leads to

$$\gamma_{10}=r_c\alpha_1+r_c^3\gamma_1+\gamma_{11}x_*^2, \quad (61)$$

$$\gamma_{20}=r_c^3\gamma_2+\gamma_{21}x_*^2. \quad (62)$$

Inserting the above equations into Eqs. (57) and (58) we obtain γ_{11} and γ_{21}, and thus $R_1(x,t)$ inside the core is completely determined:

$$\gamma_{11}=\frac{\Phi_0\Lambda_1+\Phi_1\Lambda_2}{\Phi_0^2+\Phi_1^2}, \quad (63)$$

$$\gamma_{21}=\frac{\Phi_0\Lambda_2-\Phi_1\Lambda_1}{\Phi_0^2+\Phi_1^2}, \quad (64)$$

where $\Phi_0=1-\frac{1}{2}(\mu+\frac{9}{8}\beta_rR_m^2+\frac{25}{16}\gamma_rR_m^4)x_*^2$, $\Phi_1=(\Omega+\alpha)x_*^2$, $\Lambda_1=(\beta_i/8)R_m^3+\frac{1}{2}(\mu+\frac{9}{8}\beta_rR_m^2+\frac{25}{16}\gamma_rR_m^4)(r_c\alpha_1+r_c^3\gamma_1)+(\Omega+\alpha)r_c^3\gamma_2$, $\Lambda_2=(\Delta\mu/4)R_m+(\beta_r/4)R_m^3+\frac{7}{32}\gamma_rR_m^5+\frac{1}{2}(\mu+\frac{9}{8}\beta_rR_m^2+\frac{25}{16}\gamma_rR_m^4)r_c^3\gamma_2-(\Omega+\alpha)(r_c\alpha_1+r_c^3\gamma_1)$.

B. Continuity of $\theta_{1x}(x,t)$

The continuity of $\theta_{1x}(x,t)$ at the matching point $x=x_*$ gives us the remaining two relations:

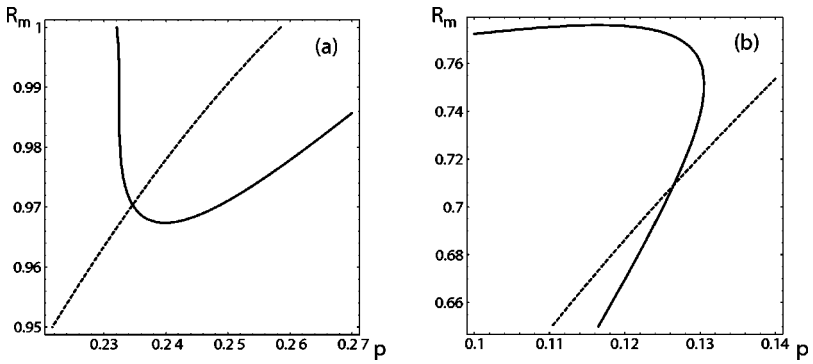

FIG. 5. (a) The intersection between the curves $f=0$ (solid line) and $g=0$ (dashed line) predicts a stable pulse. (b) The intersection between the curves $f=0$ (solid line) and $g=0$ (dashed line) predicts an unstable pulse, which plays the role of a nucleation function.

$$\delta_{20}=\beta_2-\frac{1}{p}(\epsilon_1\sqrt{p^2-\mu}-p\epsilon_2)r_c^2-\frac{\delta_{11}}{\alpha}, \tag{65}$$

$$\delta_{10}=\frac{1}{p}(\epsilon_2\sqrt{p^2-\mu}+p\epsilon_1)r_c^2+\frac{\delta_{21}}{\alpha}. \tag{66}$$

Inserting the above expressions into Eqs. (59) and (60) we obtain

$$\delta_{11}=-\frac{\alpha}{\Omega}\left\{\gamma_{10}c_{11}-c_{12}\left[\beta_2-\frac{1}{p}(\epsilon_1\sqrt{p^2-\mu}-p\epsilon_2)r_c^2\right]+d_1\right\}, \tag{67}$$

$$\delta_{21}=-\frac{\alpha}{\Omega}\left\{\gamma_{20}c_{11}+\frac{c_{12}}{p}(\epsilon_2\sqrt{p^2-\mu}+p\epsilon_1)r_c^2+d_2\right\}, \tag{68}$$

where $c_{11}=(1/2R_m)(\Omega-\mu_2+\alpha-\frac{9}{8}\beta_i R_m^2)$, $c_{12}=\Omega+\alpha$, $d_1=\Delta\mu/4+(\beta_r/8)R_m^2+\frac{3}{32}\gamma_r R_m^4$, $d_2=-(\beta_i/4)R_m^2$.

Thus we have obtained approximate analytical expressions for $R(x,t)$ and $\theta(x,t)$ in terms of R_m, p, and the parameters of the system (1) and (2).

Outside the core,

$$R(x,t)=R_0(x)+\frac{\Delta\mu}{4\mu_2}R_0(x)\sin 2[\Omega t+\theta_0(x)]+R_0^3(x)\times\{\gamma_1\sin 2[\Omega t+\theta_0(x)]+\gamma_2\cos 2[\Omega t+\theta_0(x)]\}, \tag{69}$$

$$\theta(x,t)=\theta_0(x)+\frac{\Delta\mu}{4\mu_2}\cos 2[\Omega t+\theta_0(x)]+R_0^2(x)\times\{\epsilon_1\sin 2[\Omega t+\theta_0(x)]+\epsilon_2\cos 2[\Omega t+\theta_0(x)]\}, \tag{70}$$

where $R_0(x)$ is given by Eq. (23) and $\theta_0(x)=px+p^2/2\alpha$ for $x<0$ and $\theta_0(x)=-px+p^2/2\alpha$ for $x>0$.

Inside the core,

$$R(x,t)=R_0(x)+(\gamma_{10}-\gamma_{11}x^2)\sin 2[\Omega t+\theta_0(x)]+(\gamma_{20}-\gamma_{21}x^2)\cos 2[\Omega t+\theta_0(x)], \tag{71}$$

$$\theta(x,t)=\theta_0(x)+(\delta_{10}+\delta_{11}x^2)\sin 2[\Omega t+\theta_0(x)]+(\delta_{20}+\delta_{21}x^2)\cos 2[\Omega t+\theta_0(x)], \tag{72}$$

where $R_0(x)$ is given by Eq. (19) and $\theta_0(x)=-\alpha x^2/2$.

VII. AN EXAMPLE

To see explicitly how this analytical method works we present an example. We choose the parameters $\mu_1=-0.1$, $\mu_2=1.5$, $\mu_3=-0.35$, $\beta_r=3$, $\beta_i=1$, $\gamma_r=-2.75$ and $D=1$. The intersection of the curves $f(R_m,p)=0$ given by Eq. (29) and $g(R_m,p)=0$ given by Eq. (30) leads to two pairs of (R_m,p), namely, $R_m=0.970$, $p=0.235$, and $R_m=0.709$, $p=0.126$. This situation is shown in Fig. 5.

Thus we can construct the zeroth-order approximation: $R_0(x)$ [given by Eqs. (19) and (23)] and θ_{0x} [given by Eq. (24)]. One of the pulses corresponds to a stable pulse and the other one to an unstable pulse, which is a nucleation function to pass from the zero stable solution to the stable pulse. In Fig. 6 we draw the shape and the wave vector for both pulses.

Now we focus on the stable pulse, which has $R_m=0.970$, $p=0.235$. According to Eq. (22) the frequency $\Omega=1.748$. Following the preceding section we evaluate the parameters $\alpha_1=0.0417$, $\alpha_2=0$, $\beta_1=0$, $\beta_2=0.0417$, $\gamma_1=0.3236$, $\gamma_2=-0.4483$, $\epsilon_1=0.2025$, $\epsilon_2=-0.2005$, $\gamma_{10}=0.1140$, $\gamma_{20}=-0.0440$, $\gamma_{11}=-0.0162$, $\gamma_{21}=0.0360$, $\delta_{10}=0.1349$, $\delta_{20}=0.1056$, $\delta_{11}=-0.0502$, $\delta_{21}=0.0307$.

Evaluating Eqs. (69), (70)–(72) we obtain approximate analytical expressions for $R(x,t)$ and $\theta(x,t)$ for this example. The result is a particle solution which acts as a source of traveling waves. The shape of the particlelike solution $R(x,t)$ carries out a periodic breathing motion of the maximum amplitude sending out traveling waves. This feature becomes very clear plotting $R(x,t)$ and the wave vector $\theta_x(x,t)$ in a three-dimensional plot (see Fig. 7).

Finally, a comparison between the analytical results and those obtained through direct numerical simulations has been carried out. Figure 8 shows analytical pictures for the shape and the wave vector for a fixed time. The corresponding numerical results are shown in Fig. 9. From both figures we can see that for the wave vector we have agreement within 1% for the wavelength and the amplitude of the traveling

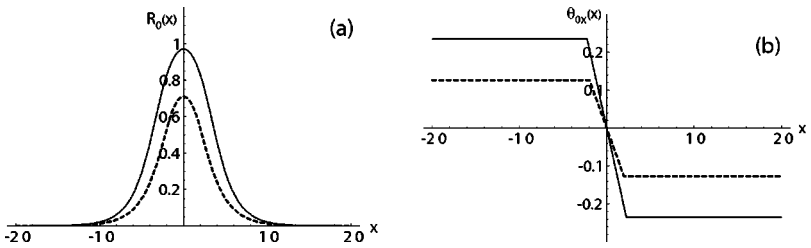

FIG. 6. Zeroth-order approximation. (a) The shape $R_0(x)$ of the stable pulse (solid line) and the shape of the unstable pulse (nucleation function) (dashed line). (b) The wave vector $\theta_{0x}(x)$ of the stable pulse (solid line) and the wave vector of the unstable pulse (dashed line).

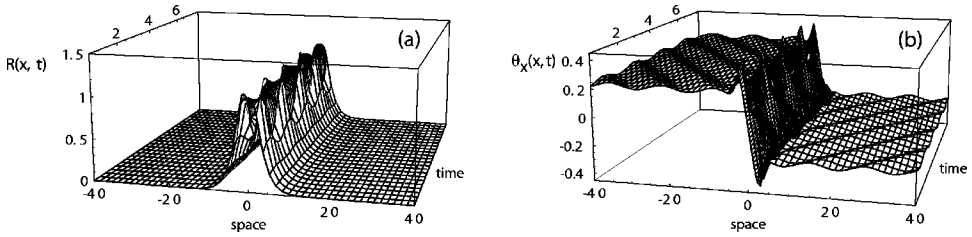

FIG. 7. Three-dimensional plot of the analytical approximation in the interval $(-40,40)\times(0.5,0.5+4\pi/\Omega)$. (a) The shape $R(x,t)$. (b) The wave vector $\theta_x(x,t)$.

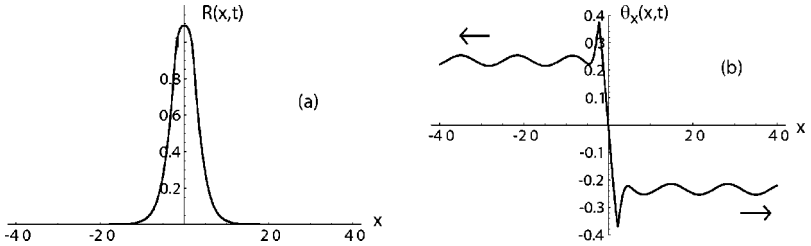

FIG. 8. Analytical results. (a) The shape $R(x,t)$. (b) The wave vector $\theta_x(x,t)$. Arrows indicate the direction of propagation of the traveling waves.

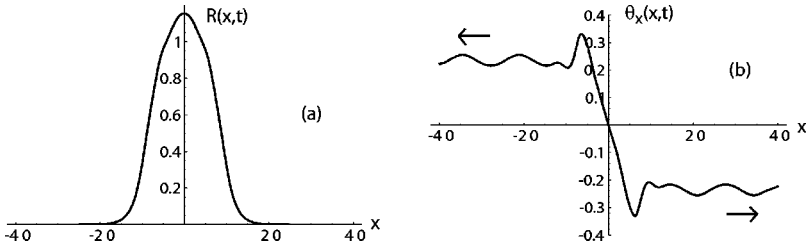

FIG. 9. Numerical results. (a) The shape $R(x,t)$. (b) The wave vector $\theta_x(x,t)$. Arrows indicate the direction of propagation of the traveling waves.

wave. For the shape of the pulse the amplitude of $R(x,t)$ coincides within 6%. These results are also true for a large range of parameters where there exist stable localized structures. Thus we conclude that the analytical shape and wave vector of the oscillating localized structure are in good agreement with those obtained by direct numerical simulations except for the width of the pulse which is a consequence of our approximative method. Nevertheless if μ_1 is near to μ_3, which is not a generic situation, the analytical and numerical shapes of the pulse (even the width) look very similar. The reason is that this class of pulses has, in this limit, more resemblance with those obtained for the Ginzburg-Landau equation and there the method works very well.

VIII. CONCLUSIONS

In this paper we have studied from an analytical point of view a simple reaction-diffusion model, which admits stable oscillating localized structures as a consequence of the coexistence between a stable limit cycle and a stable fixed point. Using a generalized matching approach, which in its simple form has been successful to obtain analytical localized structures for the subcritical (quintic) complex Ginzburg-Landau equation, we were able to find an approximate analytical expression for the oscillating pulses in this reaction-diffusion model as well. The oscillating particlelike solutions lead to the generation of traveling waves in the phase because the limit cycle is not a circle. This analytical approximation captures all the essential ingredients of these breathing particlelike solutions and is in good agreement with direct numerical simulations except for the width of the pulse.

ACKNOWLEDGMENTS

Y.H. acknowledges the Alexander von Humboldt-Foundation for financial support. H.R.B. acknowledges the Deutsche Forschungsgemeinschaft (DFG) for partial support of this work. O.D. wishes to acknowledge the support of FAI (Project Ingeniería 2004, Universidad de los Andes), FONDECYT (2004), and DFG.

[1] M.C. Cross and P. Hohenberg, Rev. Mod. Phys. **65**, 851 (1993).
[2] A.M. Turing, Philos. Trans. R. Soc. London, Ser. B **327**, 37 (1952).
[3] A. T. Winfree, *The Geometry of Biological Time* (Springer, New York, 1980).
[4] K.J. Lee, W.D. McCormick, Q. Ouyang, and H.L. Swinney, Nature (London) **369**, 215 (1994).
[5] K.J. Lee and H.L. Swinney, Phys. Rev. E **51**, 1899 (1995).
[6] J.E. Pearson, Science **261**, 189 (1993).
[7] W.N. Reynolds, J.E. Pearson, and S. Ponce-Dawson, Phys. Rev. Lett. **72**, 2797 (1994); W.N. Reynolds, S. Ponce-Dawson, and J.E. Pearson, Phys. Rev. E **56**, 185 (1997).
[8] Y. Hayase and T. Ohta, Phys. Rev. Lett. **81**, 1726 (1998).
[9] Y. Nishiura and D. Ueyama, Physica D **130**, 73 (1999).
[10] Y. Hayase and T. Ohta, Phys. Rev. E **62**, 5998 (2000).
[11] Y. Hayase and T. Ohta, Phys. Rev. E **66**, 036218 (2002).
[12] V. Petrov, K. Scott, and K. Showalter, Philos. Trans. R. Soc. London, Ser. A **347**, 631 (1994).
[13] K. Krischer and A. Mikhailov, Phys. Rev. Lett. **73**, 3165 (1994).
[14] C.P. Schenk, M. Or-Guil, M. Bode, and H.-G. Purwins, Phys. Rev. Lett. **78**, 3781 (1997).
[15] T. Ohta, J. Kiyose, and M. Mimura, J. Phys. Soc. Jpn. **66**, 1551 (1997).
[16] J. Kosek and M. Marek, Phys. Rev. Lett. **74**, 2134 (1995).
[17] Y. Hayase, J. Phys. Soc. Jpn. **66**, 2584 (1997).
[18] S. Koga and Y. Kuramoto, Prog. Theor. Phys. **63**, 106 (1980).
[19] T. Ohta, M. Mimura, and R. Kobayashi, Physica D **34**, 115 (1989).
[20] B. S. Kerner and V. V. Osipov, *Autosolitons* (Kluwer Academic, The Netherlands, 1994).
[21] T. Ohta, Y. Hayase, and R. Kobayashi, Phys. Rev. E **54**, 6074 (1996).
[22] Y. Hayase, O. Descalzi, and H. R Brand (unpublished).
[23] M. Stich, M. Ipsen, and A.S. Mikhailov, Physica D **171**, 19 (2002).
[24] O. Thual and S. Fauve, J. Phys. (France) **49**, 1829 (1988).
[25] H.R. Brand and R.J. Deissler, Phys. Rev. Lett. **63**, 2801 (1989).
[26] R.J. Deissler and H.R. Brand, Phys. Lett. A **146**, 252 (1990).
[27] S. Fauve and O. Thual, Phys. Rev. Lett. **64**, 282 (1990).
[28] W. van Saarloos and P.C. Hohenberg, Phys. Rev. Lett. **64**, 749 (1990).
[29] R.J. Deissler and H.R. Brand, Phys. Rev. A **44**, R3411 (1991).
[30] W. van Saarloos and P.C. Hohenberg, Physica D **56**, 303 (1992).
[31] R.J. Deissler and H.R. Brand, Phys. Rev. Lett. **72**, 478 (1994).
[32] R.J. Deissler and H.R. Brand, Phys. Rev. E **51**, R852 (1995).
[33] R.J. Deissler and H.R. Brand, Phys. Rev. Lett. **81**, 3856 (1998).
[34] H. Sakaguchi and H.R. Brand, Physica D **97**, 274 (1996).
[35] H. Sakaguchi and H.R. Brand, Physica D **117**, 95 (1998).
[36] K. Maruno, A. Ankiewicz, and N. Akhmediev, Physica D **176**, 44 (2003).
[37] H.R. Brand and R.J. Deissler, Phys. Rev. Lett. **63**, 508 (1989).
[38] R.J. Deissler, Y.C. Lee, and H.R. Brand, Phys. Rev. A **42**, 2101 (1990).
[39] H.R. Brand and R.J. Deissler, Phys. Rev. A **46**, 888 (1992).
[40] H.R. Brand and R.J. Deissler, Phys. Rev. E **58**, R4064 (1998).
[41] O. Descalzi, M. Argentina, and E. Tirapegui, Phys. Rev. E **67**, 015601(R) (2003).
[42] O. Descalzi, M. Argentina, and E. Tirapegui, Int. J. Bifurcation Chaos Appl. Sci. Eng. **12**, 2459 (2002).
[43] H.H. Rotermund, S. Jakubith, A. von Oertzen, and G. Ertl, Phys. Rev. Lett. **66**, 3083 (1991).